Spin-state transition in LaCoO₃ by variational cluster approximation

R. Eder

Karlsruher Institut für Technologie, Institut für Festkörperphysik, 76021 Karlsruhe, Germany

The variational cluster approximation (VCA) is applied to the calculation of thermodynamical quantities and single-particle spectra of LaCoO₃. Trial self-energies and the numerical value of the Luttinger-Ward functional are obtained by exact diagonalization of a CoO₆ cluster. The VCA correctly predicts LaCoO₃ as a paramagnetic insulator, and a gradual and relatively smooth increase in the occupation of high-spin Co³⁺ ions causes the temperature dependence of entropy and magnetic susceptibility. The single-particle spectral function agrees well with experiment; the experimentally observed temperature dependence of photoelectron spectra is reproduced satisfactorily. Remaining discrepancies with experiment highlight the importance of spin-orbit coupling and local lattice relaxation.

I. INTRODUCTION

LaCoO₃ has received considerable attention over the years because it seems to undergo two electronic transitions or crossovers in the temperature range between 50 and 600 K.[1,2] The first crossover, usually referred to as the spin state transition, can be seen most clearly in the magnetic susceptibility χ.[3–5] Below 50 K LaCoO₃ is nonmagnetic, $\chi \approx 0$, indicating that all Co³⁺ ions are in the low spin (LS) $^1A_{1g}$ or t_{2g}^6 state realized for d^6 in cubic symmetry with sufficiently large crystalline electric field (CEF). Then χ rises sharply which indicates the thermal excitation of states with nonzero spin and after a maximum around 100 K decreases again. In inelastic magnetic neutron scattering[6] the low-frequency magnetic scattering intensity near Γ shows a very similar temperature dependence as χ. A pronounced anomaly is also observed in the coefficient of thermal expansion,[6,7] the heat capacity shows only a weak anomaly at the spin state transition.[8]

Abbate *et al.*[9] found that the valence-band photoemission spectrum (PES) and O 1*s* x-ray absorbtion spectrum (XAS) show little or no change across the spin state transition. On the other hand, Haverkort *at al.*[10] found a significant temperature dependence of the Co-$L_{2,3}$ XAS and the x-ray magnetic circular dichroism spectrum (XMCD) below 500 K. Thornton *et al.*[11] observed a temperature dependence of the Co K-edge prepeak between 140 and 800 K and Medarde *at al.*[12] found that this temperature dependence sets in at 50 K, i.e., the onset of the spin state transition.

The nature of the spinful excited state which is responsible for the spin state transition has been under debate for some time. While it was proposed originally that this is the high spin (HS) $^5T_{2g}$ (or $t_{2g}^4e_g^2$) excited state of the Co³⁺ ion,[2] Korotin *et al.*[13] concluded from their (local density approximation) LDA+U calculation that this state rather is the intermediate spin (IS) $^3T_{1g}$ (or $t_{2g}^5e_g^1$) state. Recently, however, experimental evidence has accumulated[10,14–17] that it is really the HS state which is populated. This leads to a certain puzzle in that a model calculation with an A_{1g} ground state and a $^5T_{2g}$ excited state with fixed activation energy $\Delta = E(^5T_{2g}) - E(^1A_{1g})$ cannot reproduce the experimental $\chi(T)$ curve. If Δ is adjusted so as to reproduce the temperature

where χ starts to deviate from zero—≈ 50 K—the resulting maximum value of $\chi(T)$ near 100 K exceeds the experimental value by a factor of ≈ 10. The fit is much better asuming an IS excited state, which has led some authors[5,7] to conclude that an IS state is responsible for the transition.

On the other hand, Haverkort *et al.* pointed out[10] that their XAS and XMCD spectra can only be explained by admixture of a $^5T_{2g}$ excited state and concluded that the activation energy $E(^5T_{2g}) - E(^1A_{1g})$ is *temperature dependent*, rising from 20 meV at 50 K to 80 meV at 700 K (Ref. 10) and leading to a much slower increase in the population of HS ions with temperature. A somewhat puzzling feature of this scenario is that in a situation where the ground state is LS an increase in the activation energy implies an *increase* in the CEF splitting $10Dq$ with temperature. The increase[18] in the Co-O bond length—the most important parameter determining $10Dq$—with temperature, however, would result in exactly the opposite behavior. The trend thus cannot be explained in a single-ion picture but is a kind of "band effect." Kyômen *et al.*,[19,20] who deduced a very similar temperature dependence of the activation energy to reconcile magnetic susceptibility and specific-heat data, invoked a negative energy of mixing between low spin and high-spin ions.

Another reason[10] for the smaller-than-expected value of χ observed in experiment is spin-orbit coupling which splits the $^5T_{2g}$ multiplet into three levels spanning an energy of ≈ 75 meV,[16] which is large compared to the temperature where the spin state transition occurs. The lowest of these spin-orbit-split states is threefold degenerate. This low-energy triplet—itself slightly split by the trigonal distortion due to the orthorhombic crystal structure of LaCoO₃—can be identified in electron-spin resonance (ESR) (Refs. 14 and 15) and inelastic neutron scattering[16,21] experiments, whereby its g factor of $\approx 3 – 3.5$ is clear proof that it originates from a spin-orbit-split HS state rather than from an IS state.

Haverkort *et al.*[10] also found that to fit their XAS and XMCD spectra with cluster calculations they had to use a larger $10Dq$ for the A_{1g} state than for the $^5T_{2g}$ state. This hints at a participation of lattice degrees of freedom in that oxygen octahedra around HS Co³⁺ expand slightly so as to accommodate the somewhat larger radius of the HS ion. The emerging picture thus is a disordered mixture of LS and HS

states, whereby the lattice participates by an expansion of the CoO_6 octahedra around HS sites,[10] which would immediately explain the anomaly of the coefficient of thermal expansion.[6,7] As pointed out by Berggold *et al.*[23] this idea also nicely explains an anomaly in the thermal conductivity κ of $LaCoO_3$. At low temperatures the dominant contribution to κ comes from phonons and the expanded O_6 octahedra around HS Co constitute randomly distributed lattice imperfections which reduce the mean-free path of the phonons. This leads to a decrease in κ at the onset of the spin state transition and a minimum slightly below 200 K.

The idea of expanded O_6 octahedra around HS Co ions may resolve yet another puzzle, namely, the result from inelastic magnetic neutron scattering[6,21] that low-energy spin correlations in $LaCoO_3$ are ferromagnetic rather than antiferromagnetic. This is surprising in that the HS state has the configuration $t_{2g}^4 e_g^2$ so that the Goodenough-Kanamori rules would predict strong antiferromagnetic exchange interaction between two HS Co ions on nearest neighbors. The expansion of the oxygen octahedra around HS ions, however, would make the formation of HS states on nearest-neighbor Co ions energetically unfavorable so that this antiferromagnetic nearest-neighbor exchange may never have the chance to act. The ferromagnetic spin correlations could then be due to "semiconductor version" of the double exchange mechanism.[22]

Strong experimental evidence against any appreciable occupation of IS states is also provided by the EXAFS results of Sundaram *et al.*[17] These authors ruled out the existence of inequivalent Co-O bonds which would be practically inevitable in the presence of IS states because the single electron in the two e_g orbitals would make these strongly Jahn-Teller active.

The second crossover in $LaCoO_3$ is frequently referred to as a metal-insulator transition. It can be seen most clearly in the specific heat where the raw data of Stølen *et al.*[8] show a sharp "spike" at 530 K even before subtraction of the phonon background. Surprisingly for a metal-insulator transition the electrical conductivity σ does not seem to show any noticeable anomaly at this temperature. Thornton *et al.*[24] found that at low temperatures the electrical conductivity σ shows a semiconductorlike increase with temperature which can be fitted well by assuming an activation energy of $\Delta = 0.53$ eV between 380 and 520 K. There is a broad plateau between 600 and 800 K, and only above 800 K σ decreases with temperature as in a metal. Bhide *et al.*[3] fitted the temperature dependence of σ with an activation energy between 0.1–0.2 eV for temperatures below 400 K. They found a plateau between 650 and 1000 K and a decrease with temperature only above 1200 K. Thornton *et al.*[25] inferred a "high-order semiconductor-to-metal transition" between 385 and 570 K from a study of inflexion points in the σ versus T plot.

The magnetic susceptibility χ has a shallow maximum near 600 K (Refs. 3 and 4) whereas magnetic neutron scattering[6] does not show a pronounced signature of the transition. Abbate *et al.*[9] found a significant change in the O 1s XAS spectra between 100 and 570 K (Ref. 9) but the data of Thornton *et al.* (XAS at the Co K-edge) show a similar change as the O 1s XAS as the temperature changes from 140 to 300 K so this change is not necessarily related to the metal-insulator transition. Tokura *et al.* observed the filling of a gaplike structure in the optical conductivity $\sigma(\omega)$, Richter *et al.* did not observe a Fermi edge at temperatures above the crossover[26] in their photoemission spectra. The evidence for a true metal-insulator transition thus is not really compelling, and in fact Stølen *et al.*[8] considered an entirely different scenario, where the splitting of the $^5T_{2g}$ state by spin-orbit coupling plays a central rule. In this scenario, the low-temperature crossover is due to the thermal excitation of the low-energy triplet, whereas the "metal-insulator transition" corresponds the population of the remaining components.

It has been argued that the crystal structure of $LaCoO_3$ may play a role as well. In the LDA+U calculations of Korotin *et al.*[13] the structural change with increasing temperature is sufficient to induce a phase transition between magnetic and nonmagnetic ground states. Quite generally density-functional calculations show a strong sensitivity of ground-state properties to structural parameters.[29,30] An experimental result which directly shows the importance of lattice degrees of the lattice structure for the magnetic state of the Co^{3+} ion is the ferromagnetism observed recently in $LaCoO_3$ thin films under tensile strain[27] Unlike bulk $LaCoO_3$ these thin films have temperature-independent photoelectron spectra.[28]

$LaCoO_3$ clearly is a difficult problem for any kind of electronic structure calculation and has been studied by various methods during the last years: standard density-functional thory,[29] LDA+U or (generalized gradient approximation) GGA+U,[13,30–33] and dynamical mean-field theory.[34] As already mentioned LDA band-structure calculations incorrectly predict the material to be a metal in the paramagnetic state for both, the ideal perovskite structure and the true orthorombic structure.[29] Combined photoemission and bremsstrahlung isochromat spectroscopy (BIS) data[35] indicate a gap in the electronic structure although its precise magnitude is difficult to pin down because the BIS spectrum shows a slow and almost linear increase of intensity with increasing energy. Together with the satellite structures observed in valence-band photoemission[5] this indicates the importance of electronic correlations and suggests that at low temperature the material is actually a correlated insulator. From the above discussion it is moreover clear that a realistic description of the temperature dependence of the photoelectron spectra and magnetic susceptibility requires a correct description of the multiplet structure of the Co^{3+} ion and its interplay with the crystalline electric field. On the other hand the relatively small gap indicates that covalency is strong so that band effects obviously are important as well. $LaCoO_3$ therefore appears as an interesting test case for the variational cluster approximation (VCA) proposed by Potthoff.[36] This method generates trials self-energies in a finite cluster—an octahedral CoO_6 cluster in the present implementation—so that the interplay between multiplet structure and crystal-field splitting can be easily included. Being based on exact diagonalization rather than Quantum Monte Carlo the VCA can access low temperatures as necessary for the case of $LaCoO_3$. On the other hand, the present implementation is based on an LCAO fit to the band structure whose necessarily limited accuracy makes it hard to quantitatively include the effects of changes of the lattice. Therefore all calculations were car-

ried out for a rigid lattice, which for simplicity was chosen to be the s.c. ideal Perovskite structure. Bearing in mind the scenario inferred by Haverkort *et al.*—an inhomogeneous lattice distortion with CoO$_6$ octahedra expanding or contracting *locally* in response to the spin state of the Co ion—it is quite obvious that a quantitative agreement with experiment cannot be expected for any calculation for a rigid lattice. A quantitative discussion of the temperature dependence of χ moreover would require to include spin-orbit coupling which was omitted in the present study to simplify the calculations. Bearing this in mind we may expect the present calculation, with a rigid lattice and no spin-orbit coupling will reach at best qualitative agreement with experiment. As will be shown below, however, this goal is indeed achieved.

II. VARIATIONAL CLUSTER APPROXIMATION

The quantity which is subject to variation in the VCA is the electronic self-energy $\Sigma(\omega)$. More precisely the VCA seeks for the best approximation to the self-energy $\Sigma(\omega)$ of a lattice system among the subset of self-energies which can be represented as exact self-energies of a given finite cluster. The VCA is based on an expression for the grand potential Ω of an interacting many-Fermion system derived by Luttinger and Ward.[37] In a multiband system where the Green's function $\mathbf{G}(\mathbf{k}, \omega)$, the noninteracting kinetic energy $\mathbf{t}(\mathbf{k})$, and the self-energy $\Sigma(\mathbf{k}, \omega)$ for given energy ω and momentum $\mathbf{k}$ are matrices of dimension $2n \times 2n$, with n the number of orbitals in the unit cell, it reads as[38]

$$\Omega = -\frac{1}{\beta} \sum_{\mathbf{k}, \nu} e^{\omega_\nu 0^+} \ln \det[-\mathbf{G}^{-1}(\mathbf{k}, \omega_\nu)] + F[\Sigma] \quad (1)$$

where $\omega_\nu = (2\nu + 1)\pi/\beta$ with β the inverse temperature are the Fermionic Matsubara frequencies,

$$\mathbf{G}^{-1}(\mathbf{k}, \omega) = \omega + \mu - \mathbf{t}(\mathbf{k}) - \Sigma(\mathbf{k}, \omega). \quad (2)$$

with μ the chemical potential and $F[\Sigma]$ is the Legendre transform of the Luttinger-Ward functional $\Phi[\mathbf{G}]$. The latter is defined[37] as the sum of all closed linked skeleton diagrams with the noninteracting Green's functions replaced by the full Green's functions. A nonperturbative derivation of a functional with the same properties as Φ has been given by Potthoff.[39] Luttinger and Ward have shown that Ω is stationary with respect to variations in Σ,

$$\frac{\partial \Omega}{\partial \Sigma_{ij}(\mathbf{k}, \omega_\nu)} = 0, \quad (3)$$

but the crucial obstacle in exploiting this stationarity property in a variational scheme for Σ is the evaluation of the functional $F[\Sigma]$ for a given "trial Σ." Potthoff's solution[36] makes use of the fact that $F[\Sigma]$ has no explicit dependence on the single-particle terms of H and therefore is the same functional of Σ for any two systems with the *same interaction part* of the Hamiltonian. In the following only the Coulomb interaction within the Co $3d$ shell is taken into account—which is a reasonable approximation. Under this assumption $F[\Sigma]$ then is the same functional for the true perovskite lattice and for an array of identical but discon-

nected octahedral CoO$_6$ clusters. For given value of μ and β one can therefore construct trial self-energies $\Sigma(\omega)$ by exact diagonalization of a single CoO$_6$ cluster and at the same time obtain the exact numerical value of $F[\Sigma]$ by simply reverting expression (1). Here the kinetic energy $\tilde{\mathbf{t}}$ of the CoO$_6$ cluster has to be used in the Dyson equation (2). Next, the pair $(\Sigma, F[\Sigma])$ can be used in Eq. (1) for the lattice system—which simply amounts to replacing $\tilde{\mathbf{t}}$ by the kinetic energy of the lattice, $\mathbf{t}(\mathbf{k})$, in Eq. (2) and performing the $\mathbf{k}$ summation—to obtain an approximation for the grand potential of the lattice. The variation in $\Sigma(\omega)$ then is performed by varying the single-electron parameters λ_i—such as hybridization integrals or site energies—of the CoO$_6$ cluster. Condition (3) thus is replaced by the set of conditions

$$\frac{\partial \Omega}{\partial \lambda_i} = 0. \quad (4)$$

Potthoff has introduced the name "reference system" for the finite cluster used to construct trial self-energies and computing the Luttinger-Ward functional. In the present application—described in detail in Refs. 41 and 42—this is an octahedral CoO$_6$ cluster. Since it is known that exact diagonalization of clusters comprising a single transition-metal ion and its nearest-neighbor oxygens gives excellent results for the $\mathbf{k}$-integrated photoelectron spectra of many transition-metal oxides,[43–45] one may expect that the use of such a cluster as the reference system is a reasonable choice. However, different implementations of the VCA have used quite different reference systems. After being proposed by Potthoff[36] (an excellent review covering many technical details has been given by Senechal[40]) the VCA has been applied succesfully to one- and two-band Hubbard models,[46,47] to simplified models for to Fe pnictides,[48] and to transition-metal oxides with orbital degeneracy.[49]

To obtain the single-electron Hamiltonian $\mathbf{t}(\mathbf{k})$ an LDA band-structure calculation for LaCoO$_3$ was performed using the Stuttgart LMTO package. Thereby the ideal cubic perovskite structure with a Co-O bond length of 1.91 Å was assumed. The density of states (DOS) is consistent with previous results and is actually quite similar to that obtained for the correct rhombohedral structure.[29] Next, a linear combination of atomic orbitals (LCAO) fit was performed to obtain a multiorbital tight-binding parametrization of the single-electron Hamiltonian $\mathbf{t}(\mathbf{k})$. The LCAO basis comprises O $2s$ and O $2p$ orbitals at -12.834 and 0 eV, Co $4s$ and $3d$ orbitals at 19.436 and 1.731 eV and La $5p$ and $5d$ orbitals at -9.264 and 10.436 eV. For the Co $3d$ orbitals an additional $10Dq$ $= 0.848$ eV is obtained from the fit. All orbitals except O $2p$ and Co $3d$ only help to "polish" certain portions of the band structure, but to obtain a good fit they have to be included. The energies of these "auxiliary orbitals" were not subject to the fit only the respective two center integrals. These are listed in Table I. In general they refer only to nearest-neighbor bonds, but hybridization between second-nearest-neighbor oxygen has also been used. Figure 1 compares the actual LDA band structure and the LCAO fit—while the fit is not really excellent the overall band structure is reproduced reasonably well. The bands at the top of the figure which are

TABLE I. Two center integrals (in eV) obtained by a LCAO fit to paramagnetic LDA band structure of LaCoO$_3$.

	Co-O	O-O	O-O	La-O
$(sp\sigma)$	−1.504	0.000	0.000	0.000
$(pp\sigma)$	0.000	0.930	0.132	1.488
$(pp\pi)$	0.000	−0.112	0.000	−0.289
$(sd\sigma)$	−1.201	0.000	0.000	0.000
$(pd\sigma)$	1.776	0.000	0.000	−0.879
$(pd\pi)$	−0.975	0.000	0.000	0.296

absent in the LCAO band structure originate from La 5d orbitals and would require to adjust parameters such as La $(dd\sigma)$—here they are put to zero because these bands are not really interesting. In the intervals $-10 \rightarrow -7$ eV and $-4 \rightarrow 0$ eV there are bonding/antibonding bands of mixed Co 3d/O 2p character, in the intermediate energy range there are essentially nonbonding O 2p bands with very little Co 3d admixture. The deviation from LDA seems large at the R point, but it should be noted that the band top at M is also somewhat lower in the LCAO fit (the two-band structures were aligned at Γ). The total bandwidth between the maximum at M and the minimum at R is 9.48 eV for the LDA and 9.83 eV for the LCAO fit, i.e., the difference is 4% which seems tolerable.

The Coulomb interaction between Co 3d electrons is described by standard atomic multiplet theory.[50,51] More precisely the Coulomb interaction within the d shell can be written as

$$H_1 = \sum_{\kappa_1, \kappa_2, \kappa_3, \kappa_4} (\kappa_1 \kappa_2 |g| \kappa_4 \kappa_3) \quad d^\dagger_{\kappa_1} d^\dagger_{\kappa_2} d_{\kappa_3} d_{\kappa_4}. \quad (5)$$

Here we have suppressed the site label i and $\kappa = (m, \sigma)$ where $m \in \{-2, -1, \ldots 2\}$ denotes the z component of orbital angular momentum. The Coulomb matrix elements $(\kappa_1 \kappa_2 |g| \kappa_4 \kappa_3)$ are obtained by a multipole expansion of the Coulomb interaction term $1/|\mathbf{r} - \mathbf{r}|$ and involve Gaunt coefficients from the angular integrations and the three Slater-Condon parameters F^0, F^2, and F^4 from the radial integrations. The upper index thereby refers to the multipole order of the interaction and in

a d-shell is limited to ≤ 4 by the triangle condition. The somewhat lengthy complete expression for the matrix elements is given, e.g., in Eqs. (13–18)–(13–25) of the textbook by Slater.[50] F^2 and F^4 which describe higher multipole interactions can be calculated from atomic Hartree-Fock wave functions but F^0 is reduced substantially from its atomic value by solid-state screening and is treated as an adjustable parameter. In the present work the values $F^0 = 8.376$ eV, $F^2 = 10.64$ eV, and $F^4 = 6.804$ eV or, alternatively, the three Racah parameters, $A = 7.62$ eV, $B = 0.14$ eV, and $C = 0.54$ eV were used. For the lowest multiplets the full theory as described by Eq. (5) can be reduced to a parameterization in terms of a Hubbard U and Hund's rule J, which parameters then can be expressed in terms of the Slater-Condon parameters.[52] As discussed in Ref. 42 we also need to specify the "bare" d-level energy $\tilde{\epsilon}^*_d$. While the LCAO fit does give an energy ϵ_d for the Co 3d level, this contains a large contribution from the intra-d-shell Coulomb interaction. Since we want to describe this Coulomb interaction by adding Coulomb Hamiltonian (5) to the LCAO-like single-particle Hamiltonian, we have to correct for this to avoid double counting. For example, Kunes $et\ al.$[53] estimated this double-counting correction as $\tilde{\epsilon}^*_d = \epsilon_d - 9Un_d$ where n_d is the average electron number/d orbital. With a U of order 10 eV this correction obviously is large. Since first-principles calculations of screened interaction parameters are a subtle issue, however, $\tilde{\epsilon}^*_d$ was considered as an adjustable parameter in the present work and set to be $\tilde{\epsilon}^*_d = -46.4$ eV. F^0 and $\tilde{\epsilon}^*_d$ together essentially determine the magnitude of the insulating gap and the distance of the "satellite" in the photoemission spectrum from the valence-band top. With these values of the Racah parameters and $\tilde{\epsilon}^*_d$ and using Table III of Ref. 42 we obtain the energy differences $E(d^{n+1}) + E(d^{n-1}) - 2E(d^n) = A - 8B = 6.5$ eV $E(d^{n+1}\underline{L}) - E(d^n) = 1.98$ eV which are frequently referred to as the Hubbard U and the charge-transfer energy Δ. Korotin $et\ al.$[13] obtained the value $U = 7.5$ eV by density-functional calculations.

Finally, we discuss the CEF splitting $10Dq$. It is obvious, that the CEF is a crucial parameter for LaCoO$_3$ because it determines—among others—the relative energy of the A_{1g} and $^5T_{2g}$ state of the Co(3+) ion. One cannot expect that the LDA calculation and the LCAO fit will produce a sufficiently accurate estimate so as to reproduce energy scales of the
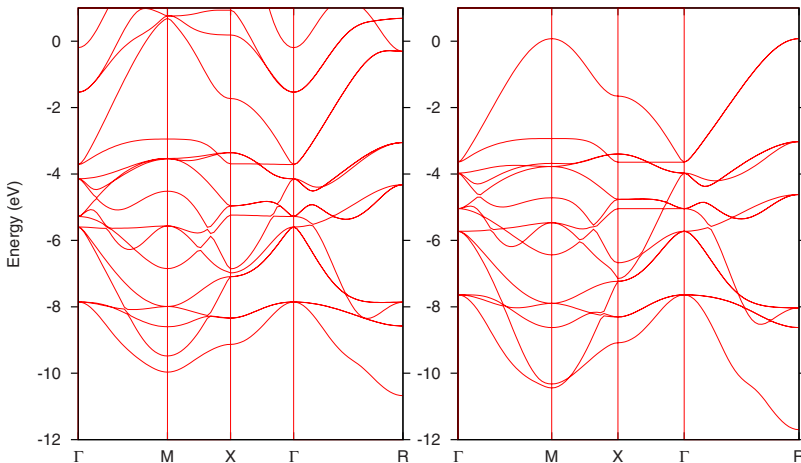

FIG. 1. (Color online) LDA band structure (left) and LCAO fit (right) for LaCoO$_3$ in the ideal Perovskite structure.

order 100 K. Therefore $10Dq$ was also treated as an adjustable parameter and to get agreement with experiment the value $10Dq=0.72$ eV was chosen, which still is rather close to the value of 0.848 eV obtained from the LCAO fit.

Next we briefly comment on the technical problem of finding a stationary point (SP) of Ω in a multidimensional parameter space. As a first step, all but one parameter λ_0 are kept fixed and λ_0 is varied until a value where $\partial\Omega/\partial\lambda_0=0$ is found. This means we are now on a surface in parameter space—which we call the "(λ_0)-surface"—where $\partial\Omega/\partial\lambda_0=0$. It is advantageous to always choose λ_0 to be the center of gravity of all orbital energies in the reference system because Aichhorn et al. showed[47] that optimization of this parameter leads to a thermodynamically consistent particle number. Then a second parameter λ_1 is chosen and varied. In each step λ_0 is recalculated to maintain $\partial\Omega/\partial\lambda_0=0$; i.e., we walk along the (λ_0) surface in parameter space while varying λ_1. The recalculation of λ_0 can be done by means of the Newton method, thereby using the solution for the preceding value of λ_1 as initial guess for the next one. Variation in λ_1 is continued until a value is found where $\partial\Omega/\partial\lambda_1=0$. This means we have now found a point of the "(λ_0,λ_1) surface" in parameter space which is defined by $\partial\Omega/\partial\lambda_0=0$ and simultaneously $\partial\Omega/\partial\lambda_1=0$. Next, we choose a third parameter, λ_2 and vary this again, walking along the (λ_0,λ_1) surface—the recalculation of λ_0 and λ_1 in each step is again done by the Newton method—until we find a point where $\partial\Omega/\partial\lambda_2=0$ and so on. This method has the advantage that it is in principle guaranteed to find a stationary point. Moreover by doing a wider scan of one parameter one can find different branches of the λ surfaces which correspond to different stationary points.

Finally we comment on the choice of the parameters to be optimized. Using the notation of Ref. 42 the four parameters ϵ_0, ϵ_1, ϵ_2, and $V(e_g)$ were varied. The values for the remaining parameters, $\epsilon_3=1.4$ eV and $V(t_{2g})=2(pd\pi)$ (Ref. 43) were kept fixed. It was checked that optimization of more than four parameters led to negligible change in Ω and very small changes in the single-particle spectral function. The reason for this "saturation" of Ω is the existence of "nearly stationary" lines in parameter space as discussed in detail in Ref. 42.

III. RESULTS

A search in parameter space for SPs of Ω revealed that for most temperatures there are actually three different SP corresponding to a d-shell occupation of ≈ 6. At low temperature the first one corresponds to the reference system being in the pure A_{1g} state, the second SP corresponds to the reference system being in a thermal mixture of an A_{1g} ground state and a $^5T_{2g}$ state at slightly higher energy, whereas the third SP corresponds to the reference system being in the pure $^5T_{2g}$ state. For "reasonable" parameters the third SP—corresponding to the HS state of the reference system—has an Ω that is substantially higher than that of the first two SP, whence this SP will never be realized. At low temperatures, on the other hand, the A_{1g}-like SP and the "mixed" SP have very similar values of Ω and for suitable choice of $10Dq$ in
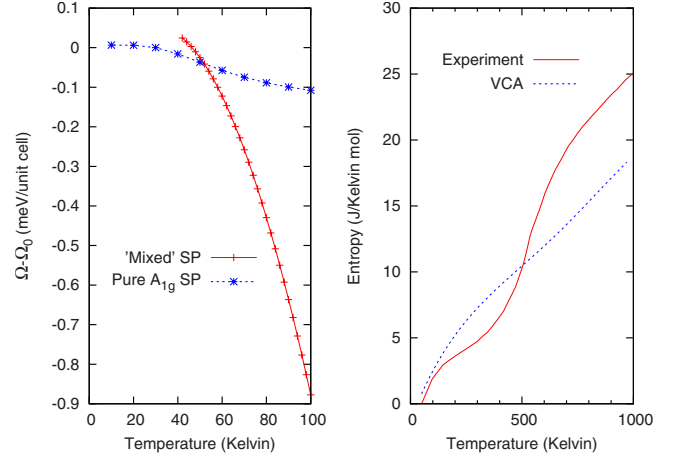

FIG. 2. (Color online) Left: grand canonical potential Ω for the two low-energy stationary points as a function of temperature. The value of $10Dq=0.72$ eV in the lattice system. Right: Entropy for the "mixed" SP as a function of temperature compared to the experimental electronic entropy found by Stølen et al. (Ref. 8).

the physical system a crossover can be seen. To illustrate this, Fig. 2 shows Ω for the A_{1g}-like and mixed SP as a function of temperature for $10Dq=0.72$ eV (the value of $10Dq$ obtained from the fit to the LMTO band structure was 0.85 eV). Accordingly this value of $10Dq$ was kept fixed for the rest of the calculation. Much unlike the cases of NiO, CoO, and MnO,[42] the parameters of the stationary points have a strong temperature dependence in the case of LaCoO₃. Obviously this reflects the subtle change with temperature of the electronic structure.

One can recognize in Fig. 2 that there is a crossing of the two $\Omega(T)$ curves at ≈ 50 K, and the finite difference in slope implies a first-order phase transition. This way of describing the spin state transition is probably an artifact of the mean-field-like description in the framework of the VCA. The latent heat for the transition would be $T\Delta S=27.8$ J/mol. It should also be noted, that the $\Omega(T)$ curve of the A_{1g}-like SP has an unphysical upward curvature above ≈ 50 K. The lower SP, however, does indeed have the correct downward curvature.

More interesting is the entropy $S(T)$ because this can be compared directly to experiment. Figure 2 shows $S(T)$ from the VCA and the experimental electronic entropy as extracted by Stølen et al.[8] from their specific-heat measurements. At low temperatures the agreement is not so bad but it is immediately obvious that the crossover at 530 K which is very pronounced in the entropy is not reproduced at all by the present calculation. This will be discussed below.

It should also be mentioned that the IS (or $^3T_{1g}$) state has negligible weight in the reference system even at the highest temperatures studied. The reason is simply the fact—already noted by Haverkort et al.[10]—that the IS state never comes even close to the ground state of the octahedral CoO₆ cluster. In that sense, the VCA complies with "LS-HS scenario" supported by experiment.[10,14–17]

Next, Fig. 3 compares the spin susceptibility from the VCA calculation to the experimental magnetic susceptibility. While the overall behavior is similar, the temperature where
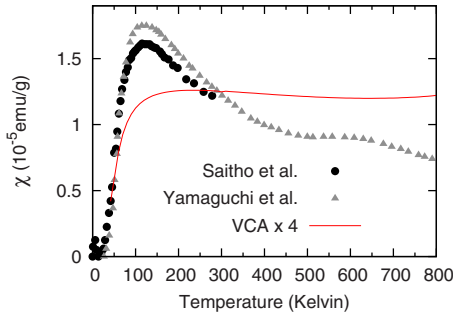
FIG. 3. (Color online) Magnetic susceptibility of LaCoO$_3$ from Refs. 4 and 5 and spin susceptibility obtained by the VCA. Note that the VCA result is multiplied by a factor of 4. The spin susceptibility in the "A_{1g}-like" SP, which is realized below 50 K, is essentially zero.

χ has its maximum does not agree with experiment and, more importantly, the calculated values are a factor ≈ 4 too small. It is likely that the reason is the rigid lattice used in the present calculation: in the actual material the expansion of the O$_6$ octahedra around a Co ion in the high-spin state probably prevents HS ions from occupying nearest neighbors so that the strong antiferromagnetic superexchange cannot act. In the VCA calculation this effect is absent, whence the antiferromagnetic nearest-neighbor exchange probably reduces the ferromagnetic spin polarization induced by the magnetic field.

One may ask for the fraction of Co ions being in the HS state. It should be noted that the VCA does not give that number for the physical system. The exact diagonalization of the reference system does give the occupation numbers of the different eigenstates of the reference system, but there is no justification for identifying these with the occupation numbers in the physical system. On the other hand, if the optimal self-energy for the lattice is realized in a cluster where the HS state has a certain weight a it is reasonably plausible that the occupation of the HS state in the physical system will not be differ completely from a. Thus, we may consider the occupation of the HS state in the reference system as a plausible estimate for the true HS occupation in the physical system. Figure 4 compares this number to experimental values. Most importantly the increase of the HS occupation with temperature is much weaker than for a system with fixed activation energy. The estimates of Haverkort *et al.* and Kyômen *et al.* are reasonably close, and also the VCA gives a roughly correct description although it obviously underestimates the HS population. This is another reason why the susceptibility computed by the VCA is too small. It is interesting, however, that the VCA gives the temperature dependence of the HS occupation at least qualitatively correct as it was carried out with a rigid lattice and therefore includes "band effects" but no effects of the local lattice relaxation.

Next we consider the occupation numbers of the various orbitals. These can be obtained for the lattice system in the standard way by integrating the spectral function of the lattice system up to the chemical potential. At 50 K, the occupation numbers/spin direction and atom for the various orbitals are $n(\text{Co } t_{2g})=2.956$, $n(\text{Co } e_g)=0.473$, and $n(\text{O } 2p)$
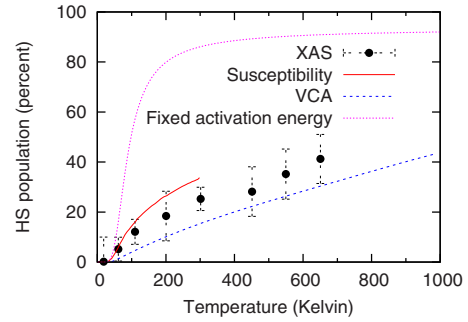

FIG. 4. (Color online) Occupation of the $^5T_{2g}$ state in LaCoO$_3$ as inferred by Haverkort *et al.* (Ref. 10) from their XAS spectra and by Kyômen *et al.* (Ref. 20) from a fit to the susceptibility and specific heat compared to the $^5T_{2g}$ occupation in the reference system for the VCA calculation. Also shown is the $^5T_{2g}$ occupation obtained with a fixed activation energy of 250 K, which reproduces the onset the spin state transition (Ref. 5).

$=2.823$. It is immediately obvious from these numbers that there is considerable charge transfer from oxygen to the e_g orbitals of cobalt. As HS Co is admixed with increasing temperature, the occupation numbers change, as can be seen in Fig. 5. The figure also shows the change of occupation numbers plotted versus the HS occupation *in the reference system*, i.e., the quantity which is shown as "VCA" in Fig. 4. The very accurate linear dependence is an indication that the HS occupation in the reference system is indeed a very good estimate for the HS occupation in the lattice system. The changes are as expected, with $n(\text{Co } e_g)$ increasing at the expense of $n(\text{Co } t_{2g})$ and a slight net charge transfer from Co to O. The nearly equal and opposite change of $n(\text{Co } t_{2g})$ and
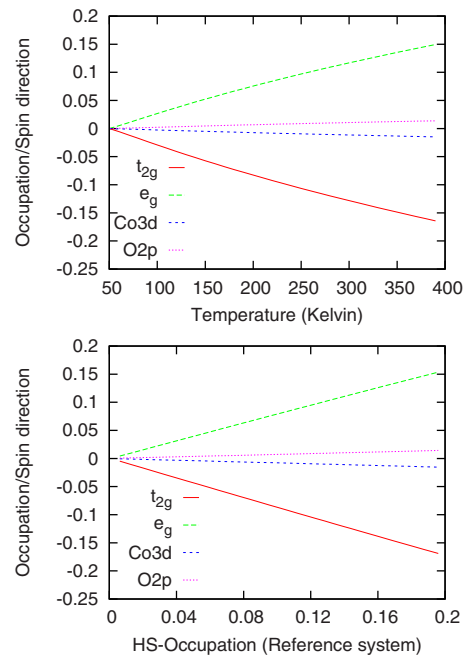

FIG. 5. (Color online) Change of occupation numbers with temperature for the "mixed" SP. The values at 50 K have been subtracted off to make changes more clearly visible. Also shown is the change of occupation numbers plotted versus HS occupation in the reference system.
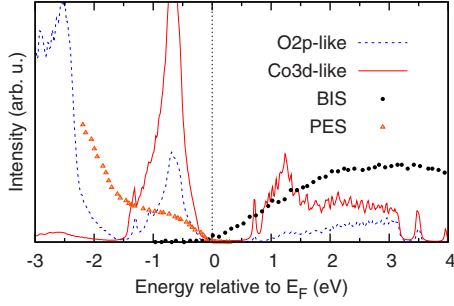
FIG. 6. (Color online) Combined PES and BIS spectra (from Ref. 35) compared to the **k**-integrated single-particle spectral function obtained from the VCA at 100 K. δ peaks are replaced by Lorentzians with a width of 0.02 eV.

$n(\text{Co } e_g)$ is expected if HS $t_{2g}^4 e_g^4$ are admixed to LS t_{2g}^6. Since the e_g orbitals hybridize with O by the stronger σ bonds and the t_{2g} by the weaker π bonds, admixture of HS states will decrease the degree of covalency hence the slight charge transfer back to oxygen. More precisely, each additional HS Co transfers 0.073 electrons to the O 2p bands.

Next, we consider the single-particle Green's function calculated with the optimal self-energy. Figure 6 shows the **k**-integrated spectral function near the Fermi energy as well as the combined PES and BIS spectra by Chainani *at al.*[35] Most importantly, the VCA correctly describes LaCoO₃ as a paramagnetic insulator—there is a clear gap of ≈ 1 eV in the spectrum. The BIS spectrum does not really show a clear edge but a gradual increase so it is hard to deduce a unique experimental gap value. The gap in the VCA spectrum of ≈ 1 eV is larger than the gap values deduced from the temperature dependence of the conductivity[3,24] which range from 0.1 to 0.53 eV (depending on temperature) or from the optical conductivity, 0.1 eV.[4] On the other hand it should be noted that the theoretical gap value does not have much real significance anyway—it is largely determined by the adjustable parameters U and Δ. More specific is the overall shape of the photoemission spectrum. Figure 7 compares the **k**-integrated spectral function with the experimental photoemission spectrum over a wider energy range. More precisely, we consider the "on-off difference" that means the difference of valence-band photoemission spectra taken with
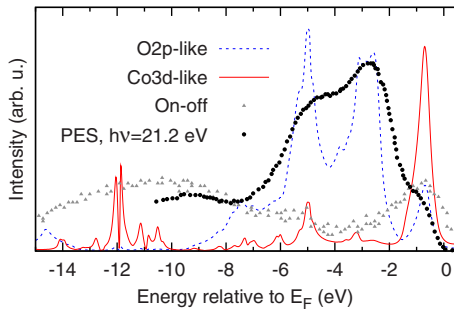

FIG. 7. (Color online) Angle integrated valence-band photoemission spectrum obtained from the VCA for the "mixed" SP at 50 K compared to the "on-off" spectrum and a photoemission spectrum taken at $h\nu=21.2$ eV (Experimental data taken from Saitho *et al.* (Ref. 5), Lorentzian broadening of the VCA specta: 0.1 eV).
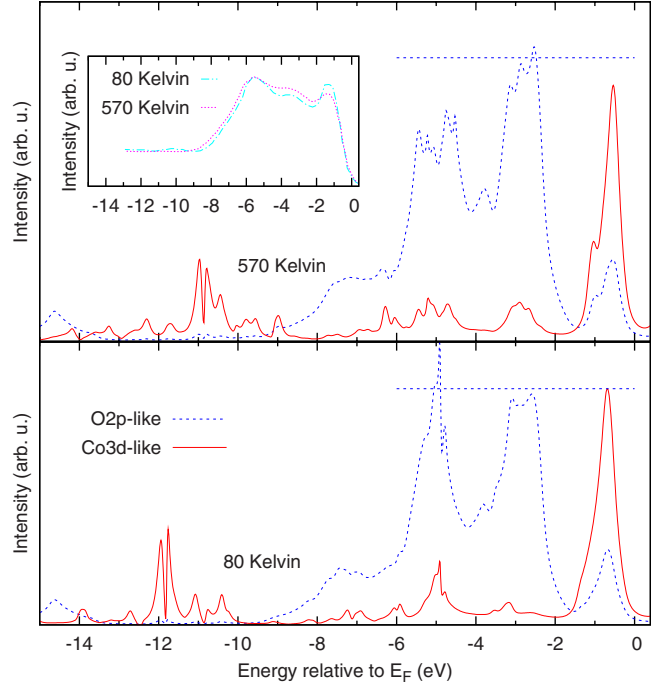

FIG. 8. (Color online) Angle integrated valence-band photoemisssion spectrum of LaCoO₃ obtained by VCA at 80 (bottom) and 570 K (top) (Lorentzian broadening 0.1 eV). The horizontal line is a guide to the eyes and corresponds to the same intensity in both spectra. The inset shows experimental spectra at different temperatures (Ref. 9).

photon energies on (63.5 eV) and slightly off (60.0 eV) the Co $3p \rightarrow 3d$ threshold, a procedure which is known[5] to emphasize the Co 3d-derived features. Also shown is a photoemission spectrum taken with a photon energy of 21.2 eV where, due to the larger photoionization cross section of the O 2p orbital[54] at this energy, mostly the oxygen derived states are visible. The VCA reproduces the main features quite accurately: the high intensity d-like peak at -1 eV, the smaller d-like peak at -5 eV and the broad "satellite" around -12 eV. Also, the three O 2p-like peaks are reproduced. The fact that the peak at the top of the valence band has predominantly Co 3d character also comes out correctly. By and large the VCA gives a reasonable description of the electronic structure of LaCoO₃, at least on coarse energy scales.

An interesting feature of LaCoO₃ is the temperature dependence of its photoelectron spectra and the VCA reproduces these at least qualitatively. Figure 8 shows the **k**-integrated spectral function at two different temperatures, 80 and 570 K. Also shown in the inset are experimental angle-integrated photoemission spectra by Abbate *et al.* As one can see in experiment the prominent peak at the top of the valence band looses weight with increasing temperature, which is a manifestation of the increasing number of Co ions in the high-spin state. The VCA reproduces this effect qualitatively, but higher temperatures are needed to obtain a similar degree of spectral weight loss. As discussed above this is simply due to the fact that the VCA underestimates the HS occupation.
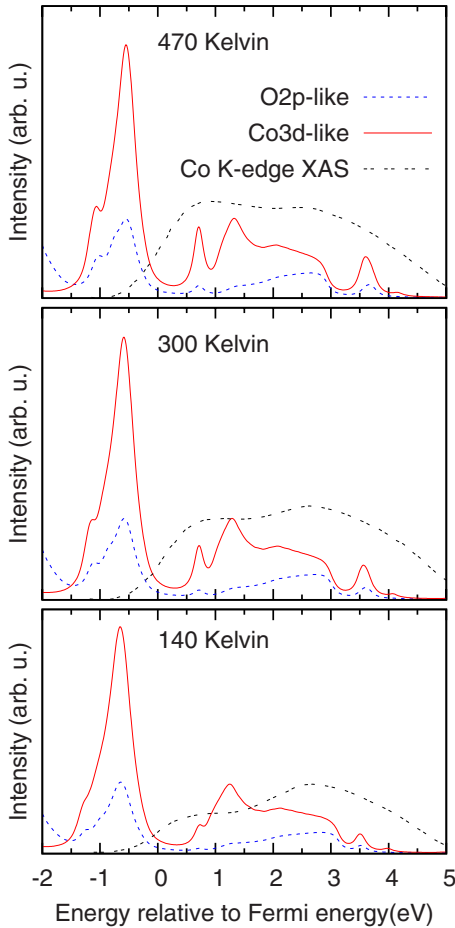
FIG. 9. (Color online) **k**-integrated single-particle spectral function from VCA at different temperatures (Lorentzian broadening 0.1 eV) compared to Co K-edge XAS spectra of $LaCoO_3$ (taken from Ref. 11). The XAS spectra have been shifted downward by ≈ 7 keV.

Next, we consider the unoccupied part of the spectrum and compare to the Co K-edge spectra by Thornton et al.[11] Figure 9 shows the spectral function at several temperatures as well as the "prepeak" of the Co K-edge spectra—shifted in energy so as to match the electron addition spectrum. The VCA spectra show a peak at ≈ 0.7 EeV above the Fermi energy which increases in intensity as the temperature increases. The experimental spectrum shows a similar change, i.e., the growing in intensity of a low-energy peak. Again, since the VCA underestimates the HS population the growth of this peak is probably underestimated. It should also be noted that the O 1s XAS spectra of Abbate et al.[9] show quite a similar behaviour as the Co K-edge spectra, namely the growth in spectral weight of a low-energy peak with increasing temperature. An apparent difference between the results of Thornton et al. and Abbate et al. is that the Co K-edge spectra seem to show a rather gradual change of the spectra with temperature, whereas the O 1s XAS spectra show little change at low temperature. The VCA gives a very continuous and gradual change as would be expected from the rather smooth increase of the HS population.

Lastly, we proceed to a comparison with other calculations on $LaCoO_3$. Several authors have calculated the DOS
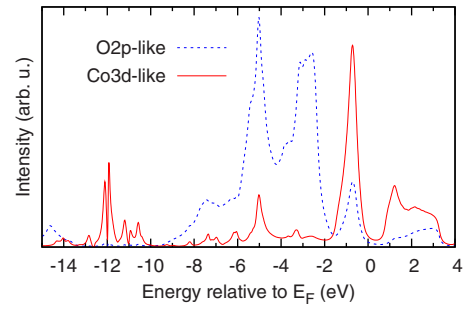

FIG. 10. (Color online) **k**-integrated single-particle spectrum obtained from the VCA for the "A_{1g}-like" SP at 10 K (Lorentzian broadening 0.1 eV).

for the low spin—or nonmagnetic—state using LDA+U or GGA+U,[13,30–33] and it may be interesting to compare the VCA to these calculations. Figure 10 shows the **k**-integrated single-particle spectrum at the lowest temperature studied, 10 K. Whereas all spectra shown so far corresponded to the "mixed SP" in Fig. 1, this spectrum is calculated for the "pure A_{1g}" SP. Despite this, one can see that the spectrum is nearly indistinguishable from the other spectra, which shows that the phase transition from the pure A_{1g} SP to the mixed SP in Fig. 1 has practically no influence on the spectrum. With the exception of the Co 3d-like "satellite" at ≈ -12 eV the spectrum is quite consistent with the GGA+U calculation of Pandey et al.[31] Especially the respective oxygen or Co character of the three prominent peaks agrees reasonably well and these agree in turn with the photon-energy dependence of the PES spectra.[5] The DOS obtained by Hsu et al.[33] shows three prominent peaks as well, but the characters do not match: there, the topmost peak has predominant oxygen character, whereas the lowermost peak has predominant Co character—this does not agree with experiment.

IV. DISCUSSION

To summarize one may say that the VCA gives a reasonably accurate description of some experimental results for $LaCoO_3$. The insulating nature of the material is described correctly and the photoelectron spectra agree with experiment in quite some detail. The temperature dependence of the magnetic susceptibility and the photoelectron spectra is reproduced at least qualitatively. For all temperatures studied only LS and HS states have appreciable weight in the density matrix of the reference system, which means that the VCA is consistent with the LS-HS scenario supported by experiment. Thereby the population of the HS states increases quite smoothly with an onset at 50 K which would be consistent with experiment as well.

The main deficiencies are the failure to reproduce the crossover seen at 530 K in the entropy and susceptibility, the too small value of the magnetic susceptibility and the too slow increase of the HS population with temperature, which makes the temperature dependence of all photoelectron spectra weaker than observed. It should be noted that changing the values of Δ and/or U so as to obtain, e.g., a smaller

insulating gap does not change this. The above deficiencies are very probably not related to an inappropriate choice of parameters.

The first reason for deviations is probably the neglect of spin-orbit coupling in the d shell. This leads to a splitting of the $^5T_{2g}$ state into a threefold, a fivefold, and a sevenfold degenerate state[14–16] which span an energy of 75 meV. If one were to assume that the activation energy in the reference system as obtained by the VCA corresponds to the center of gravity of these split states, the triplet would be appreciably lower and give a higher susceptibility and HS occupation at low temperatures. Moreover, Stølen et al.[8] considered a scenario, where the low-temperature crossover corresponds to the population of the low-energy triplet and the high-temperature transition to the population of the remaining two components. If that were indeed the case, a calculation without spin-orbit coupling could never reproduce the high-temperature transition. Since spin-orbit coupling is a single-particle term it can be included into the VCA without any problem. On the other hand the z-component of the spin is no longer a good quantum number if spin-orbit coupling is introduced, which increases the size of matrices to be diagonalized or inverted and spin-orbit coupling was neglected in the present study.

A second reason is the neglect of—or rather: the impossibility to treat—the local lattice relaxations, i.e., the expansion of O$_6$ octahedra around HS Co ions. This implies than a HS ion "feels" a different environment and that the actual activation energy has to be modified by an elastic contribution. All of these effects are missed in a calculation with a rigid lattice such as the present one. The local expansion of the O$_6$ octahedra may also have considerable impact on the magnetic susceptibility. Namely based on the Goodenough-Kanamori rules HS ions on nearest neighbors would be expected to show strong antiferromagnetic exchange via the two half-filled e_g orbitals. On the other hand, for HS ions on nearest neighbors it is clear that the respective local lattice relaxations—expansion of the O$_6$ octahedra around HS ions—would interfere with each other so that HS occupation of nearest neighbors may be energetically unfavorable and the antiferromagnetic superexchange may simply not have the chance to act. This could explain the experimental result[6,21] that low-energy spin correlations are ferromagnetic rather than antiferromagnetic as well as the surprising fact that thin films of LaCoO$_3$ under tensile order ferromagnetically.[27] In a calculation with a rigid lattice this effect would be missed so that the antiferromagnetic superexchange would reduce the spin susceptibility.

This shows that important physical effects had to be neglected in the present calculation and a quantitative agreement with experiment could not be expected. Still there is quite good qualitative agreement which demonstrates the usefulness of the VCA to study correlated insulators.

APPENDIX: CALCULATION OF THE MAGNETIC SUSCEPTIBILITIY

The magnetic susceptibility can be obtained from $\chi = -\frac{\partial^2 \Omega}{\partial B^2}$. Thereby the magnetic field B is an additional single-particle-like parameter in the physical system. The introduction of this parameter will change the stationary point; that means the parameters of the reference system become dependent on B. For the calculation of the derivative, however, we do not need to solve the optimization with applied B field.

We denote by λ_i the parameters of the reference system and by $\bar{\lambda}_i$ the values at the stationary point for $B=0$. Then we can write down the following expansion of Ω for small B:

$$\Omega = \bar{\Omega} + \frac{1}{2} \sum_{i,j} \frac{\partial^2 \Omega}{\partial \lambda_i \, \partial \lambda_j} (\lambda_i - \bar{\lambda}_i)(\lambda_j - \bar{\lambda}_j)$$
$$+ \sum_i \frac{\partial^2 \Omega}{\partial \lambda_i \, \partial B} B(\lambda_i - \bar{\lambda}_i) + \frac{B^2}{2} \frac{\partial^2 \Omega}{\partial B^2}. \tag{A1}$$

All derivatives in this equation can in principle be obtained numerically. Also it has been used that in a paramagnetic state

$$\frac{\partial \Omega}{\partial B} = 0.$$

Taking B small but finite and demanding that $\frac{\partial \Omega}{\partial \lambda_i} = 0$ we obtain

$$\sum_j \frac{\partial^2 \Omega}{\partial \lambda_i \, \partial \lambda_j}(\lambda_j - \bar{\lambda}_j) = -\frac{\partial^2 \Omega}{\partial \lambda_i \, \partial B} B.$$

We now differentiate with respect to B and set $B=0$ to obtain

$$\sum_j \frac{\partial^2 \Omega}{\partial \lambda_i \, \partial \lambda_j} \frac{\partial \lambda_j}{\partial B} = -\frac{\partial^2 \Omega}{\partial \lambda_i \, \partial B}$$

which is an equation for the derivatives $\frac{\partial \lambda_j}{\partial B}$. We assume this to be solved and thus the $\frac{\partial \lambda_j}{\partial B}$ to be known. Inserting now $\lambda_i - \bar{\lambda}_i = B \cdot \frac{\partial \lambda_j}{\partial B}$ into Eq. (A1) we obtain

$$\Omega = \bar{\Omega} + \frac{B^2}{2} \left[\frac{\partial^2 \Omega}{\partial B^2} + \sum_i \frac{\partial^2 \Omega}{\partial \lambda_i \, \partial B} \frac{\partial \lambda_j}{\partial B} \right] \tag{A2}$$

from which the susceptibility is found as

$$\chi = -\frac{\partial^2 \Omega}{\partial B^2} - \sum_i \frac{\partial^2 \Omega}{\partial \lambda_i \, \partial B} \frac{\partial \lambda_j}{\partial B}.$$

In the presence of a magnetic field all single-electron parameters of the reference system have to be taken as spin dependent, i.e., a hopping integral $t \to (t_\uparrow, t_\downarrow)$. It is then easy to see that the mixed second derivatives $\frac{\partial^2 \Omega}{\partial \lambda_i \partial B}$ are different from zero only for those λ_i which are odd under sign change of the spin; that means quantities such as $(t_\uparrow - t_\downarrow)$. At a nonmagnetic SP these are zero so the derivatives can be evaluated right at the SP.

[1] G. H. Jonker and J. H. Van Santen, Physica (Amsterdam) **19**, 120 (1953).

[2] P. M. Raccah and J. B. Goodenough, Phys. Rev. **155**, 932 (1967).

[3] V. G. Bhide, D. S. Rajoria, G. Rama Rao, and C. N. R. Rao, Phys. Rev. B **6**, 1021 (1972).

[4] S. Yamaguchi, Y. Okimoto, H. Taniguchi, and Y. Tokura, Phys. Rev. B **53**, R2926 (1996).

[5] T. Saitoh, T. Mizokawa, A. Fujimori, M. Abbate, Y. Takeda, and M. Takano, Phys. Rev. B **55**, 4257 (1997).

[6] K. Asai, O. Yokokura, N. Nishimori, H. Chou, J. M. Tranquada, G. Shirane, S. Higuchi, Y. Okajima, and K. Kohn, Phys. Rev. B **50**, 3025 (1994).

[7] C. Zobel, M. Kriener, D. Bruns, J. Baier, M. Grüninger, T. Lorenz, P. Reutler, and A. Revcolevschi, Phys. Rev. B **66**, 020402(R) (2002).

[8] S. Stølen, F. Grønvold, H. Brinks, T. Atake, and H. Mori, Phys. Rev. B **55**, 14103 (1997).

[9] M. Abbate, J. C. Fuggle, A. Fujimori, L. H. Tjeng, C. T. Chen, R. Potze, G. A. Sawatzky, H. Eisaki, and S. Uchida, Phys. Rev. B **47**, 16124 (1993).

[10] M. W. Haverkort, Z. Hu, J. C. Cezar, T. Burnus, H. Hartmann, M. Reuther, C. Zobel, T. Lorenz, A. Tanaka, N. B. Brookes, H. H. Hsieh, H.-J. Lin, C. T. Chen, and L. H. Tjeng, Phys. Rev. Lett. **97**, 176405 (2006).

[11] G. Thornton, I. W. Owen, and G. P. Diakun, J. Phys.: Condens. Matter **3**, 417 (1991).

[12] M. Medarde, C. Dallera, M. Grioni, J. Voigt, A. Podlesnyak, E. Pomjakushina, K. Conder, Th. Neisius, O. Tjenberg, and S. N. Barilo, Phys. Rev. B **73**, 054424 (2006).

[13] M. A. Korotin, S. Yu. Ezhov, I. V. Solovyev, V. I. Anisimov, D. I. Khomskii, and G. A. Sawatzky, Phys. Rev. B **54**, 5309 (1996).

[14] S. Noguchi, S. Kawamata, K. Okuda, H. Nojiri, and M. Motokawa, Phys. Rev. B **66**, 094404 (2002).

[15] Z. Ropka and R. J. Radwanski, Phys. Rev. B **67**, 172401 (2003).

[16] A. Podlesnyak, S. Streule, J. Mesot, M. Medarde, E. Pomjakushina, K. Conder, A. Tanaka, M. W. Haverkort, and D. I. Khomskii, Phys. Rev. Lett. **97**, 247208 (2006).

[17] N. Sundaram, Y. Jiang, I. E. Anderson, D. P. Belanger, C. H. Booth, F. Bridges, J. F. Mitchell, Th. Proffen, and H. Zheng, Phys. Rev. Lett. **102**, 026401 (2009).

[18] P. G. Radaelli and S.-W. Cheong, Phys. Rev. B **66**, 094408 (2002).

[19] T. Kyômen, Y. Asaka, and M. Itoh, Phys. Rev. B **67**, 144424 (2003).

[20] T. Kyômen, Y. Asaka, and M. Itoh, Phys. Rev. B **71**, 024418 (2005).

[21] D. Phelan, D. Louca, S. Rosenkranz, S.-H. Lee, Y. Qiu, P. J. Chupas, R. Osborn, H. Zheng, J. F. Mitchell, J. R. D. Copley, J. L. Sarrao, and Y. Moritomo, Phys. Rev. Lett. **96**, 027201 (2006).

[22] D. I. Khomskii and G. A. Sawatzky, Solid State Commun. **102**, 87 (1997).

[23] K. Berggold, M. Kriener, P. Becker, M. Benomar, M. Reuther, C. Zobel, and T. Lorenz, Phys. Rev. B **78**, 134402 (2008).

[24] G. Thornton, B. C. Tofield, and D. E. Williams, Solid State Commun. **44**, 1213 (1982).

[25] G. Thornton, F. C. Morrison, S. Partington, B. C. Tofield, and D. E. Williams, J. Phys. C **21**, 2871 (1988).

[26] L. Richter, S. D. Bader, and M. B. Brodsky, Phys. Rev. B **22**, 3059 (1980).

[27] D. Fuchs, C. Pinta, T. Schwarz, P. Schweiss, P. Nagel, S. Schuppler, R. Schneider, M. Merz, G. Roth, and H. v. Löhneysen, Phys. Rev. B **75**, 144402 (2007).

[28] C. Pinta, D. Fuchs, M. Merz, M. Wissinger, E. Arac, H. v. Löhneysen, A. Samartsev, P. Nagel, and S. Schuppler, Phys. Rev. B **78**, 174402 (2008).

[29] P. Ravindran, P. A. Korzhavyi, H. Fjellvåg, and A. Kjekshus, Phys. Rev. B **60**, 16423 (1999).

[30] K. Knížek, P. Novák, and Z. Jirák, Phys. Rev. B **71**, 054420 (2005).

[31] S. K. Pandey, Ashwani Kumar, S. Patil, V. R. R. Medicherla, R. S. Singh, K. Maiti, D. Prabhakaran, A. T. Boothroyd, and A. V. Pimpale, Phys. Rev. B **77**, 045123 (2008).

[32] S. K. Pandey, Ashwani Kumar, S. Banik, A. K. Shukla, S. R. Barman, and A. V. Pimpale, Phys. Rev. B **77**, 113104 (2008).

[33] H. Hsu, K. Umemoto, M. Cococcioni, and R. Wentzcovitch, Phys. Rev. B **79**, 125124 (2009).

[34] L. Craco and E. Müller-Hartmann, Phys. Rev. B **77**, 045130 (2008).

[35] A. Chainani, M. Mathew, and D. D. Sarma, Phys. Rev. B **46**, 9976 (1992).

[36] M. Potthoff, Eur. Phys. J. B **36**, 335 (2003); **32**, 429 (2003).

[37] J. M. Luttinger and J. C. Ward, Phys. Rev. **118**, 1417 (1960).

[38] J. M. Luttinger, Phys. Rev. **119**, 1153 (1960).

[39] M. Potthoff, Condens. Matter Phys. **9**, 557 (2006).

[40] D. Senechal, arXiv:0806.2690.

[41] R. Eder, Phys. Rev. B **76**, 241103(R) (2007).

[42] R. Eder, Phys. Rev. B **78**, 115111 (2008).

[43] A. Fujimori and F. Minami, Phys. Rev. B **30**, 957 (1984).

[44] F. M. F. de Groot, J. Electron Spectrosc. Relat. Phenom. **67**, 529 (1994).

[45] A. Tanaka and T. Jo, J. Phys. Soc. Jpn. **63**, 2788 (1994).

[46] M. Potthoff, M. Aichhorn, and C. Dahnken, Phys. Rev. Lett. **91**, 206402 (2003); C. Dahnken, M. Aichhorn, W. Hanke, E. Arrigoni, and M. Potthoff, Phys. Rev. B **70**, 245110 (2004).

[47] M. Aichhorn, E. Arrigoni, M. Potthoff, and W. Hanke, Phys. Rev. B **74**, 024508 (2006).

[48] M. Daghofer, A. Moreo, J. A. Riera, E. Arrigoni, D. J. Scalapino, and E. Dagotto, Phys. Rev. Lett. **101**, 237004 (2008).

[49] M. Daghofer, K. Wohlfeld, A. M. Oles, E. Arrigoni, and P. Horsch, Phys. Rev. Lett. **100**, 066403 (2008).

[50] J. C. Slater, *Quantum Theory of Atomic Structure* (McGraw-Hill, New York, 1960).

[51] J. S. Griffith, *The Theory of Transition-Metal Ions* (Cambridge University Press, London, 1964).

[52] D. van der Marel and G. A. Sawatzky, Phys. Rev. B **37**, 10674 (1988).

[53] J. Kuneš, V. I. Anisimov, A. V. Lukoyanov, and D. Vollhardt, Phys. Rev. B **75**, 165115 (2007).

[54] D. E. Eastman and J. L. Freeouf, Phys. Rev. Lett. **34**, 395 (1975).